Structural Engineering and Mechanics, *Vol. 74, No. 4 (2020) 533-545*
DOI: https://doi.org/10.12989/sem.2020.74.4.533

Optimal design of spoke double-layer cable-net structures based on an energy principle

Mingmin Ding*[1], Bin Luo[2a], Lifeng Han[3b], Qianhao Shi[4c] and Zhengxing Guo[2d]

[1]*College of Civil Engineering, Nanjing Forestry University, Nanjing 210037, Jiangsu, China*
[2]*Department of Civil Engineering, Southeast University, Nanjing 210096, Jiangsu, China*
[3]*Cob Development (Suzhou) Co. Ltd., Wuxi 214001, Jiangsu, China*
[4]*Wuxi Civil Architecture Design Institute Co. Ltd., Wuxi 214072, Jiangsu, China*

(Received June 25, 2018, Revised April 24, 2019, Accepted January 3, 2020)

Abstract. An optimal design method for a spoke double-layer cable-net structure (SDLC) is proposed in this study. Simplified calculation models of the SDLC are put forward to reveal the static responses under vertical loads and wind loads. Next, based on an energy principle, the relationship among the initial prestress level, cross-sectional areas of the components, rise height, sag height, overall displacement, and relative deformation is proposed. Moreover, a calculation model of the Foshan Center SDLC is built and optimized. Given the limited loading cases, material properties of the components, and variation ranges of the rise height and sag height, the self-weight and initial prestress level of the entire structure can be obtained. Because the self-weight of the cables decreases with increasing of the rise height and sag height, while the self-weight of the inner strut increases, the total weight of the entire structure successively exhibits a sharp reduction, a gradual decrease, a slow increase, and a sharp increase during the optimization process. For the simplified model, the optimal design corresponds to the combination of rise height and sag height that results in an appropriate prestress level of the entire structure with the minimum total weight.

Keywords: spoke double-layer cable-net; simplified calculation model; energy principle; structural optimal design; comparative analysis

1. Introduction

In the past two decades, cable-net structures have been widely used in various large-span projects (Luo *et al*. 2012) and aviation antennas (Liu *et al*. 2013, Deng *et al*. 2014). With more advanced development, more complex cable-net structures will be used to cover wider spans. For such applications, the spoke double-layer cable-net structure (SDLC) is a well-suited approach; SDLCs have been widely used in many large-span structures, such as the National Stadium in Warsaw (Fig. 1) and the Sony Center in Berlin's Potsdamer Square (Fig. 2).

Unlike traditional grid structures, cables have a relatively small bending rigidity (Vu *et al*. 2012, Wang *et al*. 2014) that is even negligible in some cases. Cables are suspended with almost no stiffness in the nontensioned state, and the initial prestress in the cables gives rigidity to

Fig. 1 National Stadium of Warsaw


Fig. 2 Sony Center in Potsdamer, Berlin

*Corresponding author, Ph.D.
E-mail: andyming1989seu@foxmail.com
[a] Associate Professor
E-mail: seurobin@seu.edu.cn
[b] Assistant Professor
E-mail: hlf426bee@126.com
[c] Civil Engineer
E-mail: 121792067@qq.com
[d] Professor
E-mail: guozx195608@126.com

ISSN: 1225-4568 (Print), 1598-6217 (Online)

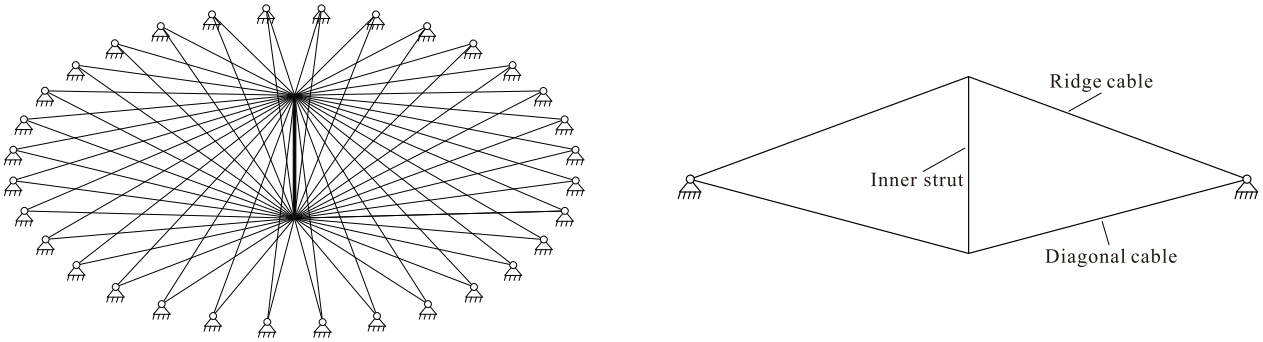

(a) Entire model (b) Calculation model of a substructure

Fig. 3 Simplified models of an SDLC

the SDLC, producing a structure with the ability to resist external loads and maintain its inherent shape. Furthermore, an SDLC has geometric nonlinearity, which leads to large variations in the structural performance from minor changes in geometry. Therefore, two key issues in the design of an SDLC are finding the initial prestress distribution and finding the initial structural shape that satisfies both the equilibrium conditions and the corresponding prestress distribution.

Currently, most of the research on structural optimal design is focused on rigid structures, and many theories have been proposed based on energy principles, e.g., the gradient-based energy minimization methods discussed by Prada and González (2014), the total potential optimization using meta-heuristic algorithms (TPO/MA) presented by Toklu *et al*. (2013), and a virtual strain energy density approach developed by Makris *et al*. (2006). However, research on the structural optimal design of prestressed spatial structures is lacking, with only limited studies (Toklu *et al*. 2017) related to cable structures.

Extensive research has been conducted on the shape and pretension optimization of tensile structures. Kawaguchi *et al*. (1999) presented a study on optimizing the maximum stiffness of a full-scale cable dome with a membrane roof. Guo and Jiang (2016) proposed a simple method for updating the geometry based on the geometrical differences under different states, and they developed a process for finding the feasible prestress of cable-strut structures. More recently, Liu *et al*. (2017) proposed a shape accuracy optimization method to find the optimal pretension for the desired shape of a cable-rib tension deployable antenna structure with tensioned cables.

A majority of the above studies involve shape and prestress optimization, and are related to the structural optimal design of SDLCs. Moreover, these methods are mainly based on the determined configuration modes of completed structures. If the locations of the cable nodes or strut nodes are unclear or change within a certain range, then the optimization simulation will be more complex. However, few studies have focused on optimization problems with this condition, and such studies have predominantly focused on antennas (Deng *et al*. 2014).

Considering the characteristics of SDLCs, the present study proposes a structural optimal design method that can be applied to SDLCs without determining the initial prestress distributions and even with unknown cable cross-sectional areas. This method proposes that the total weight of the cables and struts be used as the optimization objective and that the rise height and sag height be used as the optimization variables. By deducing the relationships among the cable forces, strut force, cross-sectional areas of the cables, rise height, and sag height, the structural optimal design of an SDLC can be obtained, including the initial prestress level, the specifications of structural components, and the initial structural shape. This optimization method is capable of producing an SDLC with a lighter self-weight and appropriate mechanical performance. Finally, a comparative analysis between the theoretical results and the FE results is conducted to verify the accuracy of this method.

2. Simplified calculation model of an SDLC

An SDLC is a tensile structure composed of n substructures (where n is a positive constant larger than one). Each substructure contains two ridge cables and two diagonal cables, with the n substructures sharing only one inner strut. In addition, all the joints between the cables and the inner strut are hinged. The simplified model of an SDLC is shown in Fig. 3(a), and the simplified calculation model of an SDLC substructure is shown in Fig. 3(b).

According to their directions, the loads on SDLCs can be divided into two categories: vertical loads (e.g., dead loads, roof live loads, or snow loads), which point down toward the ground, and wind loads (e.g., suction wind loads or pressure wind loads), which point perpendicular to the ridge cables.

Because the substructures of an SDLC are arranged radially around the inner strut at the center, the ridge cables of the SDLC bear triangularly distributed loads for both the vertical and wind loads. The detailed deformations of the SDLC are shown in Figs. 4(a)-(c), where q_v, q_{sw}, and q_{pw} are the equivalent vertical line load, the equivalent suction wind line load, and the equivalent pressure wind line load, respectively; w_v, w_{sw}, and w_{pw} are the vertical deformations of the inner strut (i.e., the mid-span displacement of the entire structure) for the vertical load condition, the suction

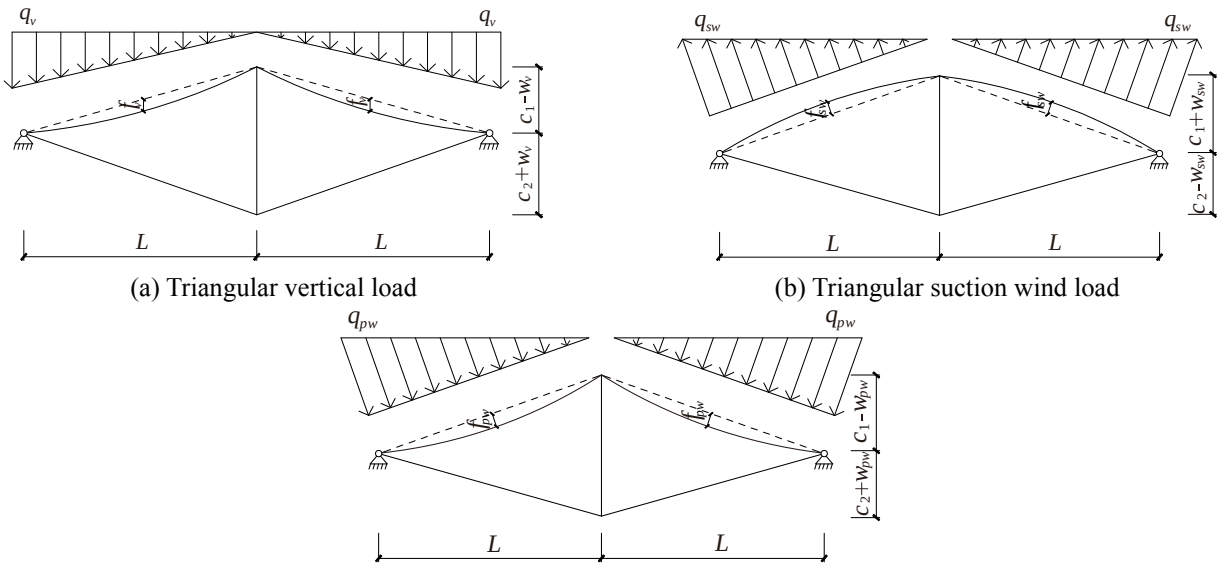

(a) Triangular vertical load

(b) Triangular suction wind load

(c) Triangular pressure wind load

Fig. 4 Deformations of an SDLC under different loads

wind load condition, and the pressure wind load condition, respectively; f_v, f_{sw}, and f_{pw} are the maximum relative deformations of the ridge cables for the vertical load condition, the suction wind load condition, and the pressure wind load condition, respectively; L is half of the span length of the entire structure; c_1 is the rise height; and c_2 is the sag height.

3. Structural performance study of SDLCs based on an energy principle

Assuming that the cables are flexible components that bear only tensile forces, the inner strut is a rigid rod that bears only compressive forces. In addition, the cables and inner strut all consist of a linear elastic material that meets the principle of superposition. Thus, the overall deformation and local deformation of an SDLC can be calculated using an energy principle.

3.1 Energy principle

For a specific cable-supported structure, several possible displacements may occur under a certain load, and these displacements must meet the structural boundary conditions. In this case, the total energy of a cable can be expressed as

$$\Pi = U + P \tag{1}$$

where Π is the total energy of a cable, U is the total strain energy of a cable with possible displacement, and P is the negative value of the virtual work imposed by the load on the possible displacement. Because the cables bear only tensile forces, only axial deformation is considered.

U is expressed as

$$U = (T_{11} + \frac{1}{2}\Delta T_1)\Delta l_1 + (T_{21} + \frac{1}{2}\Delta T_2)\Delta l_2 \tag{2}$$

$$\Delta T_1 = \frac{EA_1\Delta l_1}{l_1} \tag{3}$$

$$\Delta T_2 = \frac{EA_2\Delta l_2}{l_2} \tag{4}$$

where T_{11} and T_{21} denote the initial cable forces of the ridge cables and diagonal cables, respectively, considering only the effect of prestress; T_{12} and T_{22} denote the forces of the ridge cables and diagonal cables, respectively, considering the effects of both the prestress and external load; l_1 and l_2 denote the initial lengths of the ridge cables and diagonal cables, respectively; Δl_1 and Δl_2 denote the elongations of the ridge cables and diagonal cables, respectively; ΔT_1 and ΔT_2 denote the increments of the cable forces of the ridge cables and diagonal cables, respectively; A_1 and A_2 denote the cross-sectional areas of the ridge cables and diagonal cables, respectively; and E denotes the elastic modulus of the cables.

When adding an external load, R, the value of P is

$$P = -\sum R\Delta X \tag{5}$$

where ΔX is the increment of the real solution of the structural displacement.

Applying the principle of stationary total potential energy (Liu *et al*. 2008), Eqs. (6)-(7) can be obtained, where Eq. (7) is the static equilibrium equation of the structure:

$$\frac{\partial \Pi}{\partial w} = 0 \tag{6}$$

$$\sum_{j=1}^{n} K_{ij}\Delta X_j + R = 0, \quad i = 1,2,3.....,n \tag{7}$$

The equation for the principle of minimum potential energy (Reissner 1946) is

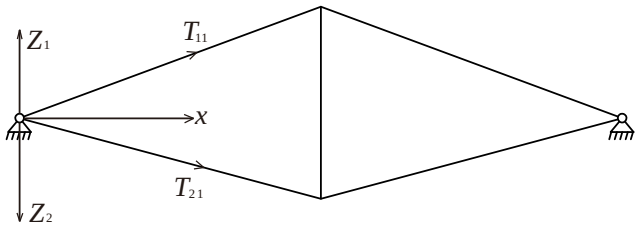

Fig. 5. Initial pretension state of the SDLC

$$\Pi(X_1)=\min\{\Pi(X)\}<\Pi(X_1+\Delta X) \tag{8}$$

where X_1 is the real solution of the structural displacement, whose total potential is the smallest among the possible displacements.

3.2 Relation between the ridge cables and diagonal cables

As shown in Fig. 5, the configuration equations of a ridge cable and a diagonal cable in the initial pretension state (i.e., considering only the forces of the cables and the inner strut) can be expressed as

$$Z_1=\frac{c_1}{L}x \tag{9}$$

$$Z_2=\frac{c_2}{L}x \tag{10}$$

where Z_1 denotes the value of the z-coordinate of the ridge cable, Z_2 denotes the value of the z-coordinate of the diagonal cable, and x denotes the value of the x-coordinate.

Assuming that the horizontal component of T_{11}, namely, H_{11}, is known, then T_{11} and T_{21} can be expressed as

$$T_{11}=\frac{H_{11}\sqrt{c_1^2+L^2}}{L} \tag{11}$$

$$T_{21}=\frac{H_{11}c_1\sqrt{c_2^2+L^2}}{Lc_2} \tag{12}$$

Then, the total potential of the cables, Π, can be expressed as

$$\begin{aligned}\Pi=&\left(\frac{H_{11}\sqrt{c_1^2+L^2}}{L}+\frac{1}{2}\frac{EA_1\Delta l_1}{l_1}\right)\Delta l_1\\&+\left(\frac{H_{11}c_1\sqrt{c_2^2+L^2}}{Lc_2}+\frac{1}{2}\frac{EA_2\Delta l_2}{l_2}\right)\Delta l_2-\sum R\Delta X\end{aligned} \tag{13}$$

The horizontal component of T_{21}, namely, H_{21}, is

$$H_{21}=\frac{H_{11}c_1}{c_2} \tag{14}$$

3.3 Structural response of SDLCs under a triangularly distributed vertical load

For SDLCs, assuming that the uniform vertical surface load applied to the roof is q_0, the value of the simplified triangular vertical load, q_v, can be expressed as

$$q_v=\frac{\pi q_0(L-x)}{n} \tag{15}$$

where n denotes the number of substructures.

The deformation of the ridge cables, u_1, can be expressed as

$$u_1=u_{11}+u_{12} \tag{16}$$

In Eq. (16), the deformation caused by w_v is

$$u_{11}=-\frac{w_v}{L}x \tag{17}$$

In Eq. (16), the deformation caused by f_v is given by

$$u_{12}=Z(x)=\frac{M(x)}{H_{12}}=\frac{\frac{L^2\pi q_0 x}{3n}-\frac{L\pi q_0 x^2}{2n}+\frac{\pi q_0 x^3}{6n}}{H_{12}} \tag{18}$$

Defining $\frac{dZ(x)}{dx}=0$, the maximum relative deformation of a ridge cable is

$$f_v=\frac{\sqrt{3}L^3\pi q_0}{27nH_{12}} \tag{19}$$

The total elongation of a ridge cable is

$$\Delta l_1=\Delta l_{11}+\Delta l_{12} \tag{20}$$

In Eq. (20), the elongation of the ridge cables caused by w_v is

$$\begin{aligned}\Delta l_{11}&=\int_0^L\left(\sqrt{1+(Z_1'+u_{11}')^2}-\sqrt{(1+(Z_1')^2}\right)dx\\&=\sqrt{L^2+(c_1-w_v)^2}-\sqrt{L^2+c_1^2}\end{aligned} \tag{21}$$

Based on Eq. (18), the elongation of the ridge cables caused by f_v is

$$\Delta l_{12}=\int_0^L\left(\sqrt{1+(Z_1'+u_{12}')^2}-\sqrt{(1+(Z_1')^2}\right)\mathrm{d}x\approx\frac{L^5\pi^2q_0^2}{90H_{12}^2n^2} \tag{22}$$

The total elongation of a ridge cable is

$$\Delta l_1=\frac{L^5\pi^2q_0^2}{90H_{12}^2n^2}+L\left(-\sqrt{1+\frac{c_1^2}{L^2}}+\sqrt{1+\left(-\frac{w_v}{L}+\frac{c_1}{L}\right)^2}\right) \tag{23}$$

The variation in the potential energy caused by the external load is

$$\begin{aligned}P&=-\sum R\Delta X\\&=-\int_0^L\left(\frac{\frac{L^2\pi q_0x}{3n}-\frac{L\pi q_0x^2}{2n}+\frac{\pi q_0x^3}{6n}}{H_{12}}\frac{\pi q_0(L-x)}{n}+\frac{w_v}{L}x\frac{\pi q_0(L-x)}{n}\right)\mathrm{d}x\\&=-\frac{L^2\pi q_0}{6n}w_v-\frac{L^5\pi^2q_0^2}{45H_{12}n^2}\end{aligned} \tag{24}$$

Combining Eqs. (6), (13), (23) and (24), w_v is

$$w_v=\frac{\frac{L^2\pi q_0}{6n}+\frac{EA_1L^5\pi^2q_0^2c_1}{90H_{12}^2n^2(L^2+c_1^2)}}{\frac{EA_1L^5\pi^2q_0^2}{90H_{12}^2n^2(L^2+c_1^2)}+\frac{EA_1c_1^2}{(L^2+c_1^2)^{1.5}}+\frac{EA_2c_2^2}{(L^2+c_2^2)^{1.5}}+\frac{H_{11}(c_1+c_2)}{Lc_2}} \tag{25}$$

3.4 Structural response of SDLCs under a triangularly distributed suction wind load

Assuming that the uniform suction wind surface load applied to the roof is q_{sw0}, the value of the simplified triangular wind load, q_{sw}, can be expressed as

$$q_{sw}=\frac{\pi q_{sw0}(\sqrt{L^2+c_1^{\,2}}-x)}{n} \tag{26}$$

The deformation caused by f_{sw} is

$$\begin{aligned}u_{12,sw}&=Z(x)\\&=\frac{M(x)}{T_{12}}\\&=\frac{2(L^2+c_1^{\,2})\pi q_{sw0}x-3\sqrt{L^2+c_1^{\,2}}\pi q_{sw0}x^2+\pi q_{sw0}x^3}{6nT_{12}}\end{aligned} \tag{27}$$

Defining $\frac{dZ(x)}{dx}=0$, the maximum relative deformation of a ridge cable is

$$f_{sw}=\frac{\sqrt{3}(L^2+c_1^2)L\pi q_{sw0}}{27nH_{12}} \tag{28}$$

Based on Eq. (27), the elongation of the ridge cables caused by f_{sw} is

$$\begin{aligned}\Delta l_{12,sw}&=\int_0^{\sqrt{L^2+c_1^{\,2}}}(Z_1'u_{12,sw}{}'+\frac{1}{2}u_{12,sw}{}'^2)\mathrm{d}x\\&=\frac{L^2(L^2+c_1^{\,2})^{\frac{3}{2}}\pi^2q_{sw0}{}^2}{90H_{12}{}^2n^2}\end{aligned} \tag{29}$$

The total elongation of a ridge cable is

$$\begin{aligned}\Delta l_{1,sw}&=\Delta l_{11,sw}+\Delta l_{12,sw}=\frac{L^2(L^2+c_1^{\,2})^{\frac{3}{2}}\pi^2q_{sw0}{}^2}{90H_{12}{}^2n^2}\\&+L(-\sqrt{1+\frac{c_1^2}{L^2}}+\sqrt{1+(-\frac{w_{sw}}{L}+\frac{c_1}{L})^2})\end{aligned} \tag{30}$$

The variation in the potential energy caused by the external load is

$$\begin{aligned}P&=-\sum R\Delta X\\&=-\int_0^{\sqrt{L^2+c_1^{\,2}}}(\frac{(L^2+c_1^{\,2})\pi q_{sw0}x}{3n}-\frac{\sqrt{L^2+c_1^{\,2}}\pi q_{sw0}x^2}{2n}+\frac{\pi q_{sw0}x^3}{6n}\frac{\pi q_{sw0}(L-x)}{n}+\frac{w_{sw}L}{L^2+c_1^{\,2}}x\frac{\pi q_{sw0}(L-x)}{n})\mathrm{d}x\\&=\frac{1}{360n^2\sqrt{L^2+c_1^2}H_{12}}L\pi q_{sw0}(\pi(L^2+c_1^2)^2(-15L+7\sqrt{L^2+c_1^2})q_{sw0}+60n\sqrt{L^2+c_1^2}(-3L+2\sqrt{L^2+c_1^2})H_{12}w_{sw})\end{aligned} \tag{31}$$

Combining Eqs. (6), (13), (30) and (31), w_{sw} is

$$w_{sw}=\frac{\frac{L^2\pi q_{sw0}}{2n}-\frac{L\pi q_{sw0}\sqrt{L^2+c_1^2}}{3n}+\frac{EA_1L^2\pi^2q_{sw0}^2c_1\sqrt{L^2+c_1^2}}{90n^2H_{12}^2}}{\frac{EA_1L^2\pi^2q_{sw0}^2\sqrt{L^2+c_1^2}}{90n^2H_{12}^2}+\frac{EA_1c_1^2}{(L^2+c_1^2)^{\frac{3}{2}}}+\frac{EA_2c_2^2}{(L^2+c_2^2)^{\frac{3}{2}}}+\frac{H_{11}(c_1+c_2)}{Lc_2}} \tag{32}$$

3.5 Structural response of SDLCs under a triangularly distributed pressure wind load

Assuming that the uniform suction wind surface load applied to the roof is q_{pw0}, the value of the simplified triangular wind load, q_{pw}, can be expressed as

$$q_{pw}=\frac{\pi q_{pw0}(\sqrt{L^2+c_1^{\,2}}-x)}{n} \tag{33}$$

Then, the maximum relative deformation of a ridge cable, f_{pw}, and the vertical deformation of the inner strut, w_{pw}, can be obtained using the same derivation process for the suction wind load condition. The detailed equations are listed as follows:

$$f_{pw}=\frac{\sqrt{3}(L^2+c_1^2)L\pi q_{pw0}}{27nH_{12}} \tag{34}$$

$$w_{pw}=\frac{\frac{L^2\pi q_{pw0}}{2n}-\frac{L\pi q_{pw0}\sqrt{L^2+c_1^2}}{3n}+\frac{EA_1L^2\pi^2q_{pw0}^2c_1\sqrt{L^2+c_1^2}}{90n^2H_{12}^2}}{\frac{EA_1L^2\pi^2q_{pw0}^2\sqrt{L^2+c_1^2}}{90n^2H_{12}^2}+\frac{EA_2c_2^2}{(L^2+c_2^2)^{\frac{3}{2}}}+\frac{EA_1c_1^2}{(L^2+c_1^2)^{\frac{3}{2}}}+\frac{H_{11}(c_1+c_2)}{Lc_2}} \tag{35}$$

3.6 Section design of ridge cables and diagonal cables

Assuming that the ridge cables and diagonal cables all reach their design strength, σ_{con}, then the tension in a diagonal cable after loading is

$$\begin{aligned}T_{22}&=A_2\sigma_{con}=T_{21}+EA_2\frac{L_2^{'}-L_2}{L_2}\\&=\frac{H_{11}c_1\sqrt{c_2^{\,2}+L^2}}{Lc_2}+EA_2\frac{\left[\sqrt{(c_2+w)^2+L^2}-\sqrt{c_2^{\,2}+L^2}\right]}{\sqrt{c_2^{\,2}+L^2}}\end{aligned} \tag{36}$$

Moreover, the horizontal component of T_{11} is

$$H_{11} = \sigma_{con} A_1 \frac{L}{\sqrt{L^2 + c_1^2}} - EA_1 \frac{L\Delta l_1}{L^2 + c_1^2} = A_1 \left(\sigma_{con} \frac{L}{\sqrt{L^2 + c_1^2}} - \frac{EL\Delta l_1}{L^2 + c_1^2} \right) \tag{37}$$

Define

$$B^* = \frac{(\sigma_{con} + E)\sqrt{c_2{}^2 + L^2} - E\sqrt{(c_2 + w)^2 + L^2}}{Ec_1 \left(c_2^2 + L^2 \right)} \tag{38}$$

Thus,

$$H_{11} = EA_2 Lc_2 B^* \tag{39}$$

In this case,

$$A_2 = A_1 \left(\frac{\sigma_{con}}{Ec_2 B^* \sqrt{L^2 + c_1^2}} - \frac{\Delta l_1}{c_2 B^* \left(L^2 + c_1^2 \right)} \right) \tag{40}$$

Assume that under the effect of both the triangularly distributed vertical load and the triangularly distributed wind load, the vertical deformation of the inner strut, w, can be calculated using Eq. (41) or Eq. (42).

Suction wind load:

$$w = \left| w_v - w_{sw} \right| \tag{41}$$

Pressure wind load:

$$w = \left| w_v + w_{pw} \right| \tag{42}$$

In addition, the maximum relative deformation of the ridge cables, f, can be calculated using Eq. (43) or Eq. (44).

Suction wind load:

$$f = \max \left\{ \left| f_v - \frac{Lf_{sw}}{\sqrt{L^2 + \left(c_1 + w_{sw} \right)^2}} \right|, \left| f_{sw} - \frac{Lf_v}{\sqrt{L^2 + \left(c_1 + w_v \right)^2}} \right| \right\} \tag{43}$$

Pressure wind load:

$$f = \max \left\{ \left| f_v + \frac{Lf_{pw}}{\sqrt{L^2 + \left(c_1 + w_{pw} \right)^2}} \right|, \left| f_{pw} + \frac{Lf_v}{\sqrt{L^2 + \left(c_1 + w_v \right)^2}} \right| \right\} \tag{44}$$

Then, combining Eqs. (19), (25), (28), (32), (34), (35), (40), (41), (42), (43), and (44), the cross-sectional areas of the ridge cable, A_1, and diagonal cable, A_2, can be obtained.

3.7 Initial prestress of the cables and inner strut

Combining Eqs. (11), (12), (16) and (36), the initial pretension of a ridge cable, a diagonal cable, and the inner strut of an SDLC are

$$T_{11} = \frac{H_{11}\sqrt{c_1{}^2 + L^2}}{L} = EA_2 c_2 B^* \sqrt{c_1{}^2 + L^2} \tag{45}$$

$$T_{21} = \frac{H_{11} c_1 \sqrt{c_2{}^2 + L^2}}{Lc_2} = EA_2 c_1 B^* \sqrt{c_2{}^2 + L^2} \tag{46}$$

$$T_{s,1} = -\frac{2nc_1}{\sqrt{L^2 + c_1{}^2}} T_{11} = -2nEA_2 c_1 c_2 B^* \tag{47}$$

where $T_{s,1}$ denotes the initial pretension of the inner strut.

3.8 Section design of the inner strut

After loading, the axial forces of the inner strut for the SDLC, $T_{s,2}$, can be expressed as follows:

Suction wind load:

$$T_{s,2} \approx -2nT_{22} \frac{c_2 + w_v - w_{sw}}{\sqrt{L^2 + \left(c_2 + w_v - w_{sw} \right)^2}} = -\frac{2nA_2 \sigma_{con} \left(c_2 + w_v - w_{sw} \right)}{\sqrt{L^2 + \left(c_2 + w_v - w_{sw} \right)^2}} \tag{48}$$

Pressure wind load:

$$T_{s,2} \approx -2nT_{22} \frac{c_2 + w_v - w_{pw}}{\sqrt{L^2 + \left(c_2 + w_v - w_{pw} \right)^2}} = -\frac{2nA_2 \sigma_{con} \left(c_2 + w_v - w_{pw} \right)}{\sqrt{L^2 + \left(c_2 + w_v - w_{pw} \right)^2}} \tag{49}$$

According to the Chinese code GB50017 (2003), the effective length factor of the struts is 1.0, and the buckling loads of these members are calculated from Eq. (50), where the maximum compressive force of a specific strut is no more than 50 % of its vertical buckling load. Thus, the cross-sectional area of a strut can be obtained by replacing the vertical buckling load, N, in Eq. (50) with $T_{s,2}$.

$$\frac{N}{\varphi A_s \sigma_y} \le 0.5 \tag{50}$$

where N, φ, A_s and σ_y are the vertical buckling load, the stability factor, the cross-sectional area and the yield strength of the inner strut, respectively.

3.9 Total self-weight of the cables and inner strut

After determining the cross-sectional areas of the cables and the inner strut, the total self-weight of the cables and inner strut can be obtained as follows:

$$Z_s = 2n\rho_{cable} \left(A_1 \sqrt{L^2 + c_1^2} + A_2 \sqrt{L^2 + c_2^2} \right) + \rho_{strut} A_s \left(c_1 + c_2 \right) \tag{51}$$

where Z_s is the total self-weight of the cables and inner strut, ρ_{cable} is the density of the cables, and ρ_{strut} is the density of the inner strut.

Therefore, the optimal initial prestress distribution (i.e., T_{11}, T_{12} and $T_{s,1}$) and the total self-weight of the cables and

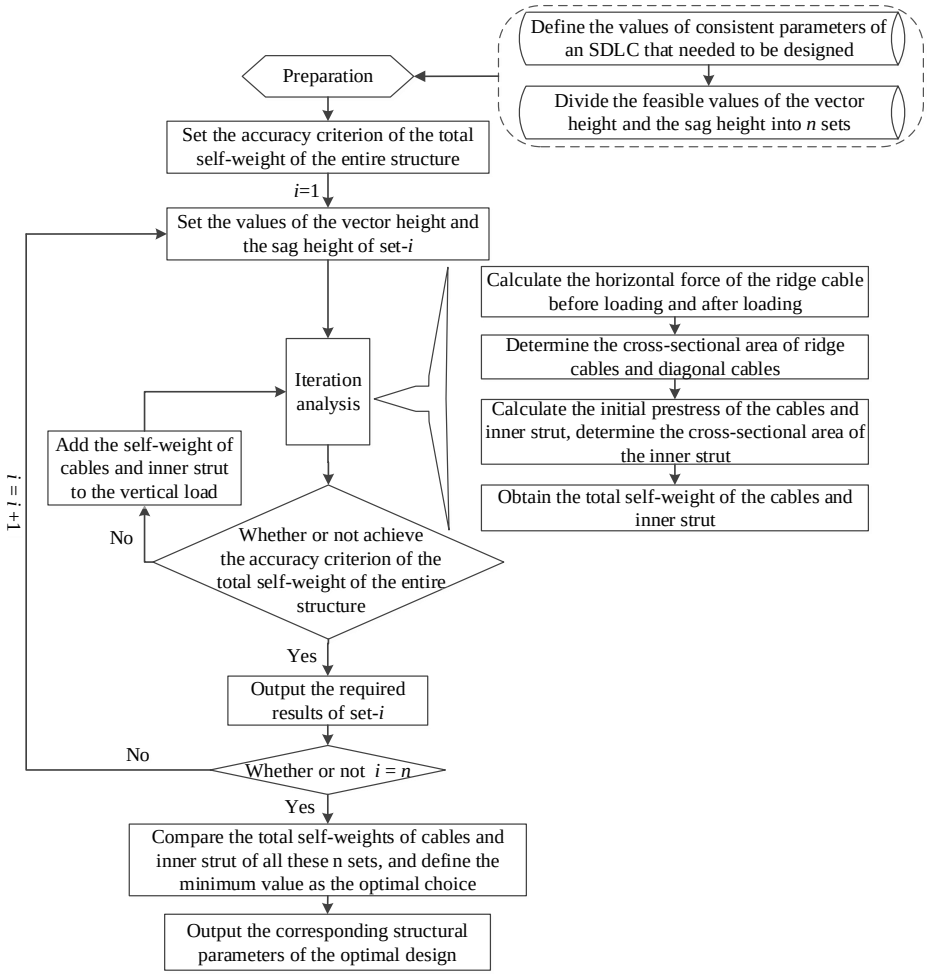

Fig. 6. Flowchart of the optimization method

strut (i.e., Z_s) of an SDLC can be derived using A_1, A_2, c_1 and c_2. Furthermore, if the values of n, L, q_0, q_{sw0}, f, w, σ_{con}, ρ_{cable}, and ρ_{strut} are known, then the optima values of A_1 and A_2 can be calculated using a given c_1 and c_2. In this case, the structural optimal design of an SDLC is related only to the variation ranges of c_1 and c_2.

4. Structural optimal design of SDLCs

4.1 Optimization objective and optimization variables

During the structural optimization of SDLCs, a suitable configuration of an SDLC must supply a sufficient reaction force to resist the external load. In addition, the self-weight of the components has a strong effect on the lengths and bearing forces of the structural components, thus determining the structural stiffness to some extent. Moreover, the weights of the cables and struts are altered during the optimization, significant affecting the economic performance of the entire structure. In this case, the total weight of the cables and struts is taken as the optimization objective.

For SDLCs, the coordinates of the cable nodes and strut nodes are important parameters that determine the geometric configuration of the entire structure. Because the roof of a building must cover a specific area, c_1 and c_2, which determine the z-coordinates of the two nodes of the inner struts, are the only variables in most cases. Furthermore, under certain boundary conditions, the level and distribution mode of the prestress strongly affect the geometric configuration, and the overall rigidity of an SDLC is related to the cross-sectional area of the cables. However, as discussed above, the optimal design of the forces and cross-sectional area of the cables can be obtained by determining the values of c_1 and c_2, and the strut can be selected afterwards. Therefore, c_1 and c_2 are chosen as the two optimization variables in this study.

4.2 Optimal design process

The specific steps of the structural optimal design are as follows:

1) Preparation for optimal design: Define the values of the constant parameters (i.e., n, L, E, q_{sw0} (or q_{pw0}), ρ_{cable}, and ρ_{strut}) and the variation ranges of c_1 and c_2 for an SDLC. Determine the uniform vertical surface load (except for the self-weight of the cables and inner strut), $q_0(0)$, the nodal displacement limit of ridge cables, f_{con}, the mid-span displacement limit of the entire structure, w_{con}, the stress

limit value of the cables, σ_{con}, and the maximum permissible variation value of the total self-weight of the entire structure, $\Delta Z_{s,lim}$.

2) Parametric decomposition: Divide the values of c_1 and c_2 into n sets (i.e., ($c_{1,1}$, $c_{2,1}$), ($c_{1,2}$, $c_{2,2}$), ($c_{1,3}$, $c_{2,3}$), …, ($c_{1,i}$, $c_{2,i}$), …, and ($c_{1,n}$, $c_{2,n}$)), and define them with the names set-1, set-2, …, set-i, …, and set-n, respectively.

3) Iteration analysis of set-i

(a) The first iteration: Define $q_0 = q_0(0)$, $c_1 = c_{1,i}$, $c_2 = c_{2,i}$, $f = f_{con}$, and $w = w_{con}$. Determine the cross-sectional areas of the ridge cables and diagonal cables based on Eqs. (19), (25), (28), (32), (34), (35), (40), (41), (42), (43), and (44), and define them as $A_{1i}(0)$ and $A_{2i}(0)$, respectively. Obtain the axial forces of the inner strut and the total self-weight of the cables and inner strut by using Eqs. (48), (49), and (51), and define them as $T_{s,2}(0)$ and $Z_{si}(0)$, respectively. Add the self-weight of the cables and inner strut to the vertical load as shown in Eq. (52). Then, define $q_0 = q_0(1)$, determine the cross-sectional areas of the ridge cables and diagonal cables based on Eqs. (19), (25), (28), (32), (34), (35), (40), (41), (42), (43), and (44), and define them as $A_{1i}(1)$ and $A_{2i}(1)$, respectively. Obtain the axial forces of the inner strut and the total self-weight of the cables and inner strut by using Eqs. (48), (49), and (51), and define them as $T_{s,2}(1)$ and $Z_{si}(1)$, respectively. Check the accuracy criterion of $\Delta Z_{si}(1)$ shown in Eq. (53).

$$q_0(1) = q_0(0) + \frac{Z_{si}(0)g}{\pi\left(L^2 + c_{1,i}^2\right)} \tag{52}$$

$$\Delta Z_{si}(1) = \left|Z_{si}(1) - Z_{si}(0)\right| \le \Delta Z_{s,\lim} \tag{53}$$

where $q_0(1)$ is the uniform vertical surface load applied to the roof, which considers the effect of the weight of the cables and inner strut in the first iteration, and g is the gravitational acceleration. In this paper, g is defined as 9.8 N/kg.

If Eq. (53) is satisfied, terminate the iteration analysis. If not, add the self-weight of the cables and inner strut to the vertical load as follows, and start the next iteration.

(b) The k^{th} iteration ($k \ge 2$): Add the self-weight of the cables and inner strut from the (k-1)th iteration to the vertical load as shown in Eq. (54). Then, define $q_0 = q_0(k)$, determine the cross-sectional areas of the ridge cables and diagonal cables based on Eqs. (19), (25), (28), (32), (34), (35), (40), (41), (42), (43), and (44), and define them as $A_{1i}(k)$ and $A_{2i}(k)$, respectively. Obtain the axial force of the inner strut and the total self-weight of the cables and inner strut by using Eqs. (48), (49), and (51), and define them as $T_{si,2}(k)$ and $Z_{si}(k)$, respectively. Check the accuracy criterion of $\Delta Z_{si}(k)$ shown in Eq. (55).

$$q_0(k) = q_0(0) + \frac{Z_{si}(k-1)g}{\pi\left(L^2 + c_{1,i}^2\right)} \tag{54}$$

$$\Delta Z_{si}(k) = \left|Z_{si}(k) - Z_{si}(k-1)\right| \le \Delta Z_{s,\lim} \tag{55}$$

where $q_0(k)$ is the uniform vertical surface load applied to the roof, which considers the effect of the weight of the cables and inner strut in the k^{th} iteration.

If Eq. (55) is satisfied, terminate the iteration analysis. If not, add the self-weight of the cables and inner strut to the vertical load as follows, and start the next iteration.

Assume that $\Delta Z_{si}(m)$ meets the accuracy condition. Then, the required cross-sectional area of the ridge cables of set-i, $A_{1i} = A_{1i}(m)$, the required cross-sectional area of the diagonal cables of set-i, $A_{2i} = A_{1i}(m)$, the axial force of the inner strut of set-i, $T_{si,2} = T_{si,2}(m)$, and the total self-weight of the cables and inner strut of set-i, $Z_{si} = Z_{si}(m)$, can be obtained. Furthermore, the required initial cable forces of the ridge cables and diagonal cables of set-i, T_{11i} and T_{21i}, respectively, can then be obtained.

4) Final computation: After the iteration analyses of all n sets, compare the total self-weights of the entire structure for each set, and define the minimum value as the optimal choice (i.e., $Z_{s,optimal}$ in Eq. (56)) and the corresponding structural parameters as the optimal structural design.

$$Z_{s,optimal} = \min\left\{Z_{s1}, Z_{s2}, ..., Z_n\right\} \tag{56}$$

The flowchart of the detailed optimal design process is illustrated in Fig. 6.

5. Example

5.1 Simplified calculation model

The roof of the Foshan Center is a typical SDLC; the roof has a span of 84 m and 64 radial pieces, i.e., the complete structure contains 64 ridge cables, 64 diagonal cables, and one inner strut (details in Figs. 7(a)-(c)). The roof is covered by membrane surface and all the cables are connected with an external support via hinged joints in three directions (x-coordinate, y-coordinate, and z-coordinate). All the cables have a density of 7.85×10^3 kg/m^3, an elastic modulus of 1.95×10^5 MPa, and a design strength (σ_{con}) of 928 MPa. The inner strut has a density of 7.85×10^3 kg/m^3, an elastic modulus of 2.06×10^5 MPa, and a yield strength (σ_y) of 310 MPa.

5.2 External load and load distributions

The external load consists of four parts: the dead load (D'), roof live load (L'), wind load (W'), and initial pretension load (P'). The dead load includes the weights of all the structural components and the weight of the membrane roof system. The total weight of all the structural components, Z_s, is calculated after each iteration and is added to the structural weight. The weight of the membrane roof system is assumed to be 0.10 kN/m^2. The roof live load is equivalent to 0.50 kN/m^2. The relevant provision in the Load Code for the Design of Building Structures GB 50009 (2012) indicates that the basic wind pressure is w_0 = 0.50 kN/m^2, the surface roughness is B, the wind-pressure height coefficient is μ_z = 1.5, the wind vibration coefficient is β_z = 1.8, and the shape coefficient is μ_s = 0.8. Thus, the wind suction load (W') is $w_k = \beta_z\mu_s\mu_z w_0$ = 1.08 kN/m^2. Moreover, the initial pretension load (P') is obtained from the optimization results.

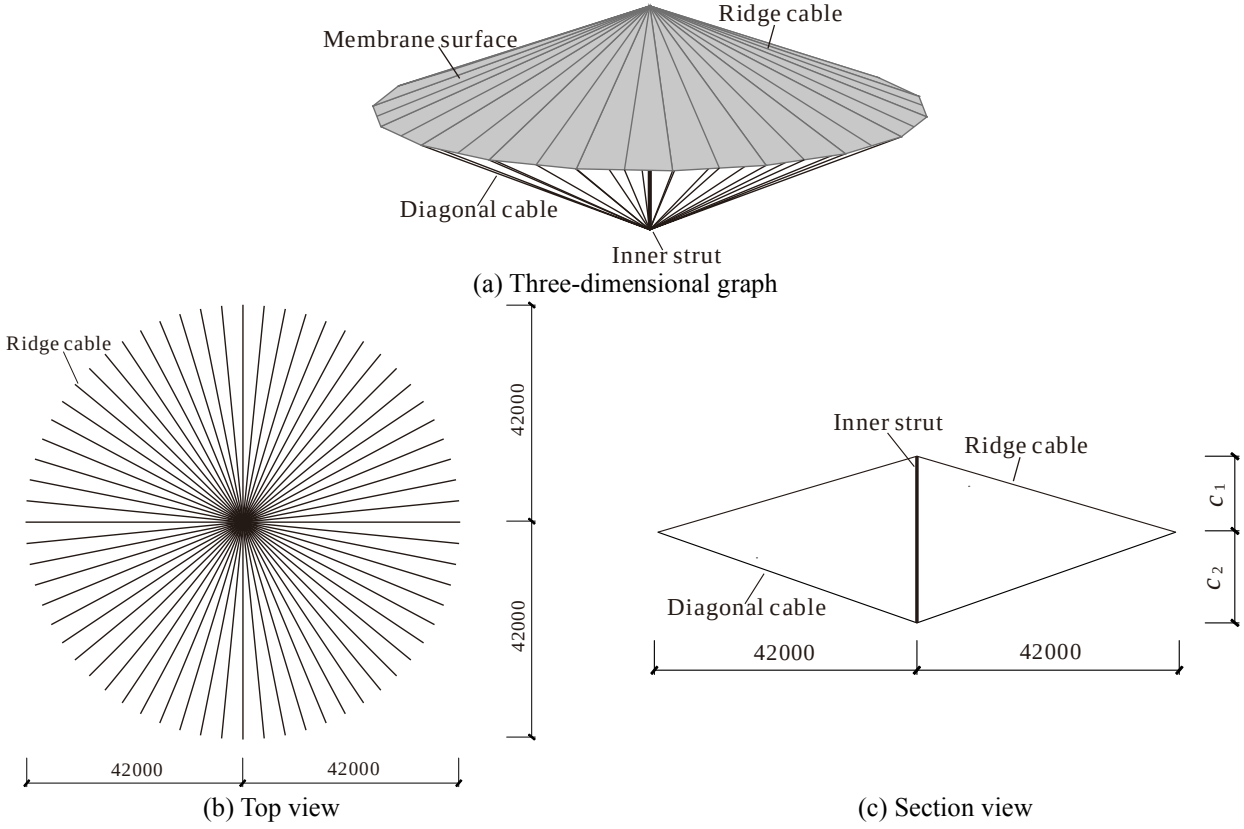

(a) Three-dimensional graph

(b) Top view

(c) Section view

Fig. 7. Simplified calculation model of the Foshan Center

Table 1 Load cases

Name	Load case
LC-1	1.2D’ + 1.4L’ + 1.0P’
LC-2	1.0D’ + 1.0L’ + 1.0P’
LC-3	1.0D’ + 1.4W’ + 1.0P’
LC-4	1.0D’ - 1.4W’ + 1.0P’

There are four load cases considered in this study, as listed in Table 1. LC-1 and LC-2 consider the effects of the vertical loads and initial pretension. Cases LC-3 and LC-4 additionally consider the suction wind load and pressure wind load, respectively, to consider the combined effect of the vertical load and wind load. For convenience, the weights of the membrane roof system, roof live load, snow load, and wind load are simplified as line loads applied on the cables of the simplified model.

5.3 Limiting factors

During the structural optimal design analysis, the cross-sectional dimensions of the cables are constantly changed to determine the optimal structure for a specific roof load. To guarantee the bearing capacity is met under diverse load cases, the optimal structural models must comply with the following limiting factors:

1) The maximum relative displacement of the ridge cables, f, must be restricted to the range of [0, $\sqrt{L^2+c_1^2}$ /100] (i.e., $f_{\text{con}}=\sqrt{L^2+c_1^2}$ /100), and the mid-span displacement of the whole structure, w, must be restricted to [0, L/500] (i.e., $w_{con}=L/500$).

2) The values of c_1 and c_2 both vary in the range of [1000 mm, 21000 mm], as suggested by experts at the conference held for the Foshan Center.

3) The maximum stress of a specific cable should be less than its design strength.

5.4 Result of the optimization analysis

Figs. 8(a)-(b) show the contour map of the self-weight of the cables and that of the inner strut of LC-1, respectively. As shown in these figures, given the design values of L, σ_{con}, q_0, q_{sw0} (or q_{pw0}), f_{con}, and w_{con}, with increasing c_1 and c_2, the self-weight of all the cables significantly decreases, whereas the self-weight of the inner strut increases because the geometric stiffness of the structure increases with increasing rise-to-span and sag-to-span ratios. In this case, the prestress level of the entire structure decreases with increasing c_1 and c_2, thus reducing the cross-sectional areas of the cables. However, with increasing c_1 and c_2, the lengths of the cables also increase, resulting in a slow decrease in the self-weight of the cables during the last stage of Fig. 8(a). In contrast, with increasing c_1 and c_2, the slenderness ratio of the inner strut increases, reducing the stability factor and increasing the cross-sectional area of the inner strut, as indicated in Eq. (50); these effects sharply increase the self-weight of the inner strut.

Fig. 8(c) displays the contour map of the total self-weight of the entire structure, Z_s, for LC-1. As stated above,

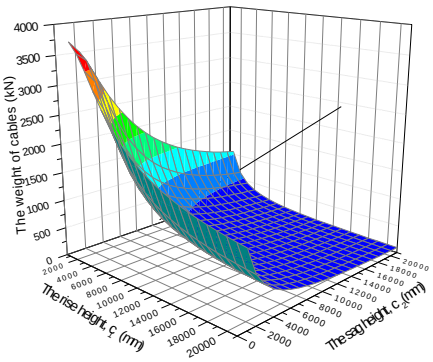

(a) Total self-weight of all the cables

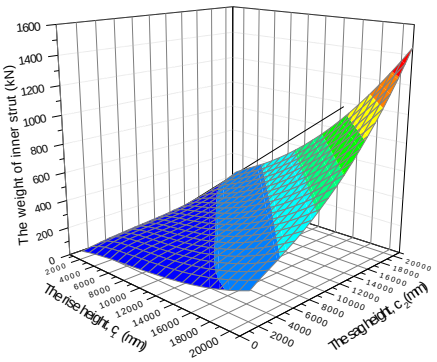

(b) Self-weight of the inner strut

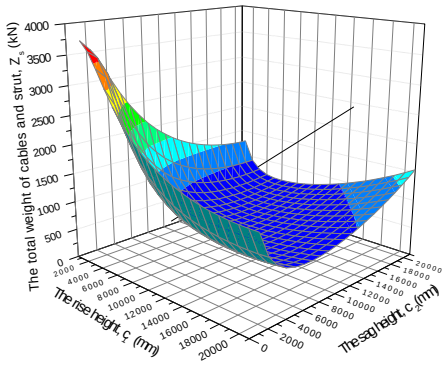

(c) Total self-weight of the entire structure, Z_s

Fig. 8. Contour maps of LC-1

Z_s is large for small values of c_1 and c_2 during the initial stage because of the large pretension forces of the cables. With increasing c_1 and c_2, the prestress level of the entire structure decreases along with Z_s. However, when the value of Z_s reaches a critical point, the self-weight of the inner strut significantly increases, and Z_s increases again. In this case, the optimal mode of the SDLC for LC-1 is the corresponding combination of c_1 and c_2 at the critical point in Fig. 8(c) that results in a suitable slenderness ratio of the inner strut, an appropriate prestress level of the entire structure, and the minimum value of Z_s.

Fig. 9(a) illustrates the variation of Z_s with various values of c_1 ($1000 \le c_1 \le 21000$) for LC-1, and Fig. 9(b) shows the variation of Z_s with various values of c_2 ($1000 \le c_2 \le 21000$) for LC-1. The results reveal that the variation of Z_s exhibits four stages under a vertical load. For a consistent value of c_2 (or c_1), Z_s decreases sharply from a relatively high point during the initial increasing stage of c_1 (or c_2) and then starts to decrease gradually in the second stage. After reaching a critical point, Z_s slowly increases during the third stage. Finally, the increasing slope of Z_s accelerates, and a sharp increase in Z_s occurs in the last stage.

For LC-1, the critical value of Z_s occurs at $c_1 = 10000$ mm in Fig. 9(a) and at $c_2 = 12000$ mm in Fig. 9(b), which is the optimal combination of c_1 and c_2, and the following parameters can be obtained: $A_1 = 618.96$ mm^2, $A_2 = 608.39$ mm^2, inner strut dimensions of 730 mm × 35 mm, $T_{11} = 595.07$ kN, $T_{21} = 501.71$ kN, and $Z_s = 526.83$ kN.

Similarly, the optimal combinations of c_1 and c_2 for the other load cases can be obtained by the above calculation process, and the corresponding results are listed in Table 2.

Table 2 Optimal modes of the calculation model under different load cases

Load case	LC-1	LC-2	LC-3	LC-4
c_1 (mm)	10000	9000	10000	11000
c_2 (mm)	12000	11000	11000	14000
A_1 (mm^2)	618.96	542.69	773.46	943.65
A_2 (mm^2)	608.39	514.14	818.25	903.52
Dimensions of the inner strut (mm)	730 × 35	670 × 30	740 × 35	780 × 40
T_{11} (kN)	595.07	517.56	744.75	914.23
T_{21} (kN)	501.71	428.02	680.85	732.47
Z_s (kN)	526.83	421.06	593.92	822.27

The results of LC-1 and LC-2 indicates that the vertical loads greatly affect the optimal modes of SDLCs. A larger total value of the vertical loads (i.e., LC-1) requires a relatively large rise height (i.e., c_1) and sag height (i.e., c_2) to increase the overall stiffness; thus, the initial pretension forces of the cables, the cross-sectional areas of the cables, the dimensions of the inner strut, and the total self-weight of the entire structure are larger. In addition, when considering the effect of wind loads, the direction of the wind is extremely important. A pressure wind load increases the total value of the downward load, increasing the vertical deformation of the inner strut and the relative deformations of the ridge cables, whereas the vertical loads offset part of the effect of the suction wind load. In this case, the structural parameters (i.e., c_1, c_2, A_1, A_2, T_{11}, T_{21}, Z_s, and the dimensions of the inner strut) of the optimal mode with

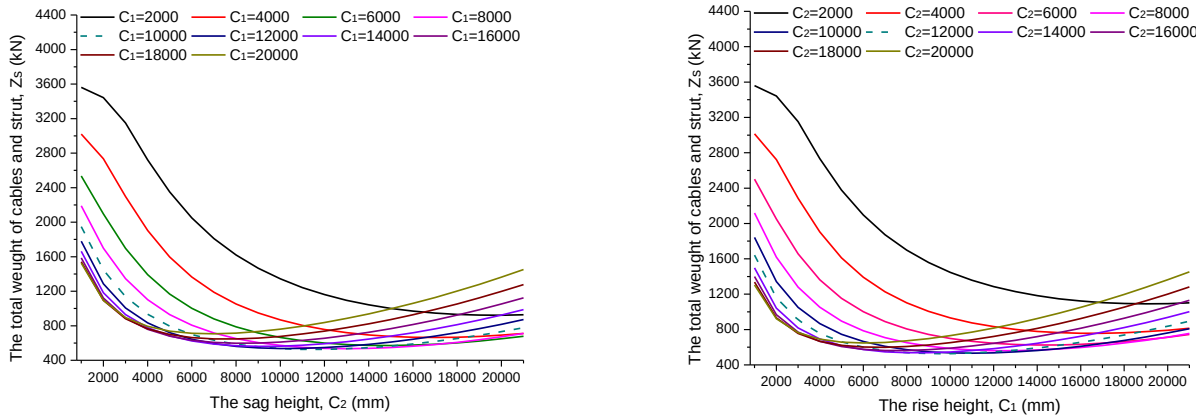

(a) Variation of Z_s with various values of c_1 ($1000 \le c_1 \le 21000$) (b) Variation of Z_s with various values of c_2 ($1000 \le c_2 \le 21000$)

Fig. 9. Variation of the total self-weight of the entire structure, Z_s, for LC-1

Table 3 Parameters of the final optimal structure

c_1 (mm)	c_2 (mm)	A_1 (mm^2)	A_2 (mm^2)	Dimensions of the inner strut (mm)	T_{11} (kN)	T_{21} (kN)	Z_s (kN)
11000	14000	943.65	903.52	780 × 40	914.23	732.47	822.27

pressure wind are relatively large. After a comprehensive review of the above four optimal modes, the parameters of the final optimal structure are selected and are listed in Table 3 to meet the requirements of all four load cases.

5.5 Comparison of the theoretical solution and FE solution

To verify the accuracy of the optimization method proposed in this study, a numerical model is built in ANSYS with parameters that match those of the final optimal structure listed in Table 3. The initial pretension forces of the cables are determined by adding an equivalent strain.

The three-dimensional two-node cable element LINK10 is chosen for the ridge cables and diagonal cables. The three-dimensional linear finite strain beam element BEAM188 is chosen for the inner strut. The three-dimensional structural surface effect element SURF154 is selected for the roof. The ridge cables and diagonal cables are all meshed into 30 elements to simulate the local deformation, the inner strut is meshed into four elements to consider the buckling condition, and the roof is meshed into 60 divisions along the radial direction and 64 divisions along the circumferential direction to share the same nodes with the ridge cables and to transfer the load added to the roof. Two loads (i.e., the vertical load, q_{v0}, and the suction wind load, q_{sw0}) are added to the model, both with a range of 0.1-1.0 kN/m^2.

Tables 4-5 show the total potential energies and the values of w_v, f_v, w_{sw}, and f_{sw} with the variations of the two loads, respectively. The largest difference in the vertical displacement between the theoretical and FE values is -1.94 mm, the largest difference in the relative deflection of the ridge cables is 8.25 mm, and the largest difference in the

Table 4 Total potential energies and downward displacements of the final optimal structure under vertical load

Vertical load (kN/m^2)	Present theoretical method			FE method		
	w_v (mm)	f_v (mm)	Total potential energy (kN.m)	w_v (mm)	f_v (mm)	Total potential energy (kN.m)
0.1	2.77	26.21	31788.76	2.47	23.83	31827.70
0.2	5.61	49.51	31805.68	4.92	45.94	31781.67
0.3	8.52	72.90	31743.75	7.37	68.55	31729.38
0.4	11.20	96.30	31714.22	9.82	90.69	31671.52
0.5	13.86	119.69	31633.35	12.27	112.37	31607.83
0.6	16.75	146.84	31521.34	14.93	143.24	31530.56
0.7	20.98	171.27	31501.14	19.8	169.66	31461.19
0.8	24.59	195.79	31429.55	23.06	196.83	31402.70
0.9	27.28	220.37	31382.55	26.43	224.7	31343.57
1.0	31.85	245.01	31353.59	29.91	253.26	31283.53
Maximum difference				-1.94	8.25	-70.06

Table 5 Total potential energies and upward displacements of the final optimal structure under suction wind load

Suction wind load (kN/m^2)	Present theoretical method			FE method		
	w_{sw} (mm)	f_{sw} (mm)	Total potential energy (kN.m)	w_{sw} (mm)	f_{sw} (mm)	Total potential energy (kN.m)
0.1	1.64	14.23	32083.23	1.89	16.33	32055.58
0.2	3.3	29.2	32115.49	3.78	33.03	32085.14
0.3	4.99	44.61	32101.13	5.67	49.73	32110.14
0.4	6.7	60.39	32106.39	7.56	66.43	32130.59
0.5	8.44	76.57	32109.16	9.45	83.13	32146.48
0.6	10.21	92.99	32108.81	11.34	99.84	32157.80
0.7	12	109.85	32157.98	13.23	116.53	32165.72
0.8	13.87	126.1	32190.89	15.11	133.23	32166.80
0.9	15.78	145.06	32194.12	17.69	151.33	32163.07
1.0	17.52	161.67	32221.01	18.89	166.64	32157.56
Maximum difference				1.91	6.27	-63.45

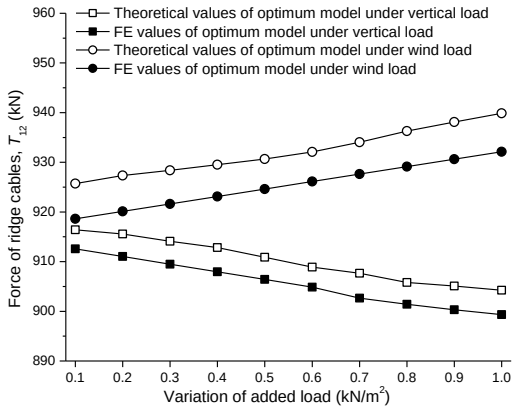

Fig. 10 Load-T_{12} diagram

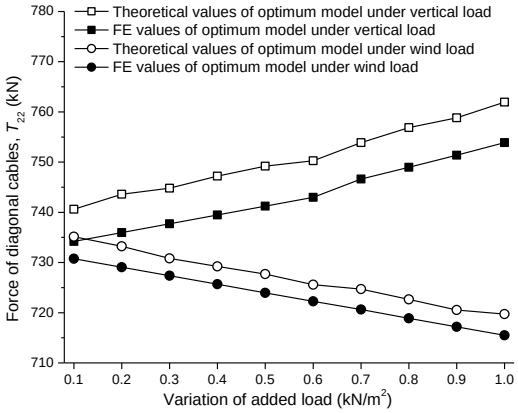

Fig. 11 Load-T_{22} diagram

total potential energy value of the final optimal structure is -70.06 kN.m; all of these values were obtained with a vertical load of 1.0 kN/m^2. The values of T_{12} and T_{22} with the variations of the two loads are presented in Figs. 10 and 11. The errors between the theoretical and FE values of the cable forces are within 8.07 kN. Thus, the theoretical solution is confirmed to ensure the accuracy of the optimization analysis.

6. Conclusion

This study presented a structural optimal design method for SDLCs taking the rise height and sag height as the optimization variables and taking the total weight of the cables and inner strut as the optimization objective. The simplified calculation model of the SDLC was proposed to reveal the structural characteristics and static response. Furthermore, the relationships among the initial component forces, cross-sectional areas of the cables, rise height, sag height, overall displacement and local displacement were proposed based on an energy principle. Given the load cases, displacement limits, design strength of the cables, and buckling criteria of the inner strut, the initial prestress level of the entire structure, the cross-sectional areas of the cables, and the specification of the inner strut can be obtained by simply determining the rise height and sag height. A simplified model of a typical SDLC project was built and optimized, and a comparative analysis between the theoretical results and the FE results was conducted to verify the accuracy of this method. The following conclusions were drawn:

1. The structural optimal design method for an SDLC proposed in this study is accurate and efficient.

2. The values of rise height and sag height significantly affect the self-weight of the components and the initial prestress level of an SDLC. In particular, when the combination of these two values is suitable, the material properties of the cables and the inner strut are fully used, reducing the total weight.

3. With increasing rise height and sag height, the geometric stiffness of the entire structure increases, decreasing the prestress level, cable cross-sectional areas, and cable self-weight. However, during this process, the cable lengths also increase, gradually decreasing the cable self-weight at large values of rise height and sag height. Moreover, with increasing rise height and sag height, the slenderness ratio of the inner strut increases, reducing the stability factor and increasing the cross-sectional area of the inner strut and thus sharply increasing the self-weight of the inner strut.

4. Because the self-weight of the cables decreases with increasing self-weight of the inner strut, the total self-weight of the entire structure exhibits four stages with increasing rise height and sag height: a sharp reduction during the initial stage, a subsequent gradual decrease in the second stage, a slow increase in the third stage, and a sharp increase in the last stage. The optimal mode of the SDLC is the corresponding combination of the rise height and sag height that results in a suitable slenderness ratio of the inner strut, an appropriate prestress level of the entire structure, and the minimum total self-weight of the entire structure, which appears between the second stage and the third stage.

5. A larger total value of the vertical loads needs a larger rise height and sag height to increase the overall stiffness; thus, the initial pretension forces and the dimensions and self-weight of the structural components are larger. Furthermore, because the vertical loads counteract part of the suction wind load, the structural parameters of the optimal mode for the pressure wind condition are relatively larger than those for the suction wind condition.

Acknowledgments

The authors acknowledge the financial support of the National Natural Science Foundation of China (Grants No 11673039), the Natural Science Foundation of Jiangsu Province (Grants No BK20190753), the Natural Science Foundation of the Jiangsu Higher Education Institutions of China (Grants No 18KJB560011), and the Priority Academic Program Development of Jiangsu Higher Education Institutions (PAPD).

References

Deng, H., Li, T., Wang, Z. and Ma, X. (2014), "Pretension Design of Space Mesh reflector antennas based on projection principle",

J. Aerosp. Eng., **28**(6), 04014142. https://doi.org/10.1061/(ASCE)AS.1943-5525.0000483.
GB 50017 (2003). Code for design of steel structures, China Architecture & Building Press; Beijing, China.
GB 50009 (2012), Load code for the design of building structures, China Architecture & Building Press; Beijing, China.
Guo, J. and Jiang, J. (2016), "An algorithm for calculating the feasible pre-stress of cable-struts structure", *Eng. Struct.*, **118**, 228-239. https://doi.org/10.1016/j.engstruct.2016.03.058.
Kawaguchi, M., Tatemichi, I. and Chen, P.S. (1999), "Optimum shapes of a cable dome structure", *Eng. Struct.*, **21**(8), 719-725. https://doi.org/10.1016/S0141-0296(98)00026-1.
Liu, F., Li, H.J. and Wang, T.C. (2008), "Energy principle and nonlinear electric–mechanical behavior of ferroelectric ceramics", *Acta Mech.*, **198**(3-4), 147-170. https://doi.org/10.1007/s00707-007-0530-0.
Liu, R.W., Guo, H.W., Liu, R.Q., Wang, H.X., Tang, D.W. and Song, X.K. (2017), "Shape accuracy optimization for cable-rib tension deployable antenna structure with tensioned cables", *Acta Astronaut.*, **140**, 66-77. https://doi.org/10.1016/j.actaastro.2017.07.047.
Liu, W., Li, D.X. and Jiang, J.P. (2013), "Mesh topological form design and geometrical configuration generation for cable-network antenna reflector structures", *Struct. Eng. Mech.*, **45**(3), 411-422. https://doi.org/10.12989/sem.2013.45.3.411.
Luo, X.Q., Zhang, Q.L. and Chen, L. (2012), "Form-finding of a mixed structure with cable nets and tubular trusses", *J. Constr. Steel. Res.*, **72**(4), 192-202. https://doi.org/10.1016/j.jcsr.2011.12.005.
Makris, P.A., Provatidis, C.G. and Venetsanos, D.T. (2006), "Structural optimization of thin-walled tubular trusses using a virtual strain energy density approach", *Thin Wall. Struct.*, **44**(2), 235-246. https://doi.org/10.1016/j.tws.2006.01.005.
Prada, A.D.L. and González, M. (2014), "Assessing the suitability of gradient-based energy minimization methods to calculate the equilibrium shape of netting structures", *Comput. Struct.*, **135**,128-140. https://doi.org/10.1016/j.compstruc.2014.01.021.
Reissner, E. (1946), "Analysis of shear lag in box beams by the principle of the minimum potential energy", *Q. Appl. Math.*, **4**(3), 268-278.
Toklu, Y.C., Bekdas, G. and Temur, R. (2017), "Analysis of cable structures through energy minimization", *Struct. Eng. Mech.*, **62**(6): 749-758. https://doi.org/10.12989/sem.2017.62.6.749.
Toklu, Y.C., Bekdas, G. and Temur, R. (2013), "Analysis of trusses by total potential optimization method coupled with harmony search", *Struct. Eng. Mech.*, **45**(2), 183-199. https://doi.org/10.12989/sem.2013.45.2.183.
Vu, T.V., Lee, H.E. and Bui, Q.T. (2012), "Nonlinear analysis of cable-supported structures with a spatial catenary cable element", *Struct. Eng. Mech.*, **43**(5), 583-605. https://doi.org/10.12989/sem.2012.43.5.583.
Wang, L., Wu, Y. and Wang, D. (2014), "Thermal effect on damaged stay-cables", *J. Theor. App. Mech-pol.*, **52**(4), 1071-1082. https://doi.org/10.15632/jtam-pl.52.4.1071.